

Achieving Shear Wave Elastography by a Three-element Probe for Wearable Human-machine Interface

Jipeng Yan, Xingchen Yang, Xiaowei Zhou, Mengxing Tang, Honghai Liu

Abstract—Shear elastic modulus of skeletal muscles can be obtained by shear wave elastography (SWE) and has been linearly related to muscle force. However, SWE is currently implemented using array probes. Price and volumes of these probes and their driving equipment prevent SWE from being used in wearable human-machine interfaces (HMI). Moreover, beamforming processing for array probes reduces the real-time performance. To achieve SWE by wearable HMIs, a customized three-element probe is adopted in this work, with one element for acoustic radiation force generation and the others for shear wave tracking. In-phase quadrature demodulation and 2D autocorrelation are adopted to estimate velocities of tissues on the sound beams of the latter two elements. Shear wave speeds are calculated by phase shift between the tissue velocities. Three agar phantoms with different elasticities were made by changing the weights of agar. Values of the shear elastic modulus of the phantoms were measured as 8.98, 23.06 and 36.74 kPa at a depth of 7.5 mm respectively. This work verifies the feasibility of measuring shear elastic modulus by wearable devices.

Keywords—Shear elastic modulus, skeletal muscle, ultrasound, wearable human-machine interface.

I. INTRODUCTION

A core of the human-machine interface (HMI) technique is to obtain information which can characterize human motions or intentions. Then, the information can be applied to build models of body or control various devices. Joint motions are driven by skeletal muscles. Any sensing method that can characterize skeletal muscles has the potential to be used for HMIs. Ultrasound waves can penetrate muscles non-invasively and the waves reflected from the interfaces in muscles carry the information of muscles. Although ultrasound has been widely used in medical imaging for several decades, research of ultrasound-based HMI has only begun in recent years.

Morphological information of skeletal muscles can be obtained by B-mode ultrasound images. Muscle thickness, volume as well as fascicle length [1], pinnation angle [2] and curvature [3], [4] have been related to joint angles or torque.

This work was supported by the National Natural Science Foundation of China (Grant Nos. 51575338, 61733011).

Yan and Yang are with the State Key Laboratory of Mechanical System and Vibration, School of Mechanical Engineering, Shanghai Jiao Tong University, Shanghai, 200240, China (e-mail: jipengyan@sjtu.edu.cn, xingchen.yang@sjtu.edu.cn).

Zhou and Tang are with the Department of Bioengineering, Imperial College London, London, SW7 2AZ, UK (e-mail: xiaowei.zhou@imperial.ac.uk, mengxing.tang@imperial.ac.uk)

Liu is with the State Key Laboratory of Robotics and System, School of Mechanical Engineering and Automation, Harbin Institute of Technology, Shenzhen, 518052, China and with the School of Computing, University of Portsmouth, Portsmouth, PO1 3HE, UK (corresponding author, e-mail: honghai.liu@icloud.com).

However, B-mode images are generated using linear or convex array probes. These probes and their driving equipment are bulk and expensive. HMI based on B-mode ultrasound is far from wearable applications, such as prostheses and exoskeleton. Therefore, HMI based on A-mode ultrasound has been studied. Similar with the B-mode counterpart, muscle thickness was found to be in high correlation with joint angles [5]. In our previous work, four single-element transducers were used to recognize hand gestures [6]. An online classification accuracy of more than 95% was achieved by processing envelopes of ultrasound which mapped the morphological information. But it is found that morphological information detected by A-mode ultrasound performed better in classifying hand gestures but worse in estimating force, in comparison to the surface electromyography [7]. In case of adding additional types of sensors in HMI, it is necessary to find other information that can be obtained by ultrasound and can characterize skeletal muscles.

Due to the development of ultra-fast ultrasound imaging, shear wave elastography (SWE) came true. The principle of SWE is to calculate the shear elastic modulus by tracking the generated shear waves and measuring the shear wave speeds. Shear elastic modulus obtained by SWE has been related to joint torque or muscle force in both *in vivo* [8]–[10] and *in vitro* experiments [11]. As the shear waves are generated by acoustic radiation force, the propagating direction of the shear waves is approximately vertical to the sound beam. Namely, the high lateral resolution is necessary for tracking the shear waves. Thus, SWE is mostly based on B-mode images, where the high lateral resolution can be achieved via beamforming processing. As mentioned above, probes and equipment for ultrasound imaging are not suitable for many wearable applications of HMI. Moreover, beamforming processing is time-consuming and will reduce the real-time performance of HMIs if embedded in HMIs. Moreover, the high-frame-rate imaging using an array probe, whose elements are usually 128 or more, generates masses of data. Currently, most of wearable devices can not transfer and store large amounts of data with enough efficiency.

To measure shear elastic modulus of skeletal muscles by wearable devices, a customized three-element transducer is adopted in this work to realize SWE. Moreover, the beamforming processing is eliminated from the data processing. Thus, the lateral resolution of three-element transducer depends on the diffraction of ultrasound. Manually-made phantoms with different elasticities are

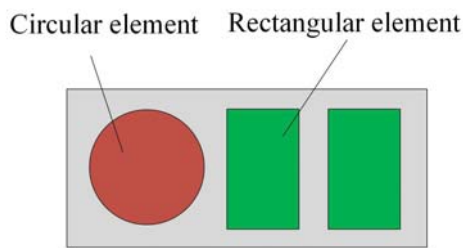


Fig. 1 Probe consists of one circular and two rectangular elements

used in the experiment. Results verify the feasibility of detecting shear elastic modulus by wearable HMIs.

II. MATERIALS AND METHODS

A. Data Acquisition

1) Probe. As shown in Fig. 1, the probe consists of three elements and the center frequencies of three elements are all 5 MHz. The circular element with diameter of 7 mm is used for generating acoustic radiation force and shear waves. The other two rectangular elements with length of 6 mm and width of 4 mm are used for tracking the shear waves. The distance between the centers of the two rectangular elements is 5 mm.

2) Phantoms. Three tissue-mimicking phantoms were manually made with different elasticities and used as targets of measurements. The components of phantoms are agar, silica and water. Their elasticities differ for the weights of agar in them, which are 1 %, 1.5 % and 2 % respectively. The silica serves as scatters and its weights in all the phantoms are 1 %. The phantoms were made by the following steps:

- stirring and heating the water to 90 °C with agar added slowly;
- keeping stirring and cooling down the solution to 55 °C with silica added slowly;
- filtering the solution with a sieve;
- leaving the solution at least 4 hours for degassing;
- storing the mixture in a fridge.

During degassing and storage, the surfaces of the phantoms were covered with a little water to prevent water in the phantoms from evaporation.

3) Equipment. The circular element is joined to a wave generator (33250A, Agilent, CA) and a power amplifier (240L, Electronics & Innovation, NY) to get a mechanical index (MI) of 1.2 at the focus. The length of pushing waves is set to 200 μ s. Two rectangular elements are connected to a Verasonics system (Vantage 128, Verasonics, WA) and the pulse repetition frequency (PRF) is set to 10 kHz. The wave generator and Verasonics system are timed by a trigger and the wave generator is controlled by the triggerout” process of the Verasonics system. All the elements are excited at their center frequency and the sampling frequency of Verasonics systems is set to 20 MHz. Each phantom is measured for ten times.

B. Data Processing

1) Estimating tissue velocity. A shear wave can be tracked by the vibration of tissues on its propagating path. Tissues

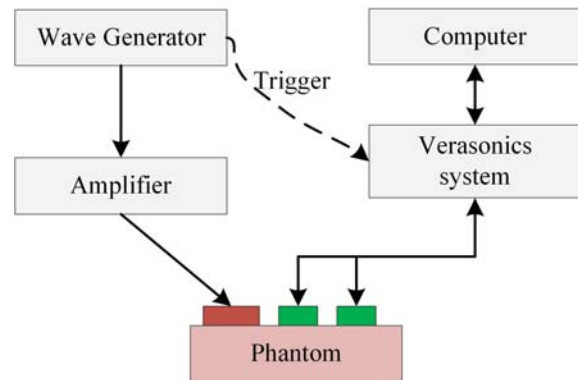


Fig. 2 The circular element and two rectangular elements are used to generate and track shear waves respectively

oscillate vertically to the propagating direction of the shear wave. Namely, the direction of the tissue vibration is along the depth direction when the shear wave transmit along the lateral direction. Therefore, the tissue vibration can be detected by Doppler methods. The transient tissue velocities v can be estimated by the 2D autocorrelation (1) [12], where F_s is the pulse repetition frequency, f_s the sampling frequency, c the speed of the longitudinal wave.

Equation (1) is based on complex demodulated signals. Considering that the two-channel analog signals are generated by piezoelectric elements and digitalized by the Verasonics system as real values, in-phase and quadrature demodulation is applied on the two-channel signals to get I and Q values for (1). Because the sampling frequency is quadruple of the center frequency of elements, the normalized demodulation frequency f_{dem} in (1) is 0.25. The sampling lengths of the 2-D autocorrelation in the fast-time (M) and slow-time (N) are set to 16 and 10, respectively, with a slide step of the range gate along the depth direction set to 1. Then, transient tissue velocities on the sound beam corresponding to each element can be obtained.

2) Calculating shear modulus. Transient tissue velocities are filtered by a low-pass filter with a cutoff frequency of 1000 Hz, in order to remove high-frequency jitter from the temporal velocity profiles. Next, the velocities are windowed and averaged over 50 samples along the depth direction (about 1.875 mm) to improve the signal to noise ratio (SNR). The averaged data are denoted by the initial depths of corresponding windows. Then, the shear wave speed c_t is calculated through dividing the distance between the centers of two elements by the time delay between two particle velocity curves. Finally, the shear modulus μ is calculated by [13]

$$\mu = \rho c_t^2 \quad (2)$$

where ρ is the density of the phantoms. Means and standard deviations of ten measurements of each phantom are calculated. To evaluate the stability of measuring the shear elastic modulus at different depths, the standard deviations versus depths are normalized by their corresponding means respectively.

$$v = \frac{c}{2} \frac{\frac{f_s}{2\pi} \tan^{-1} \left(\frac{\sum_{m=0}^{M-1} \sum_{n=0}^{N-2} [Q(m,n)I(m,n+1) - I(m,n)Q(m,n+1)]}{\sum_{m=0}^{M-1} \sum_{n=0}^{N-2} [I(m,n)I(m,n+1) + Q(m,n)Q(m,n+1)]} \right)}{\frac{f_s}{2\pi} \left(2\pi f_{dem} + \tan^{-1} \left(\frac{\sum_{m=0}^{M-2} \sum_{n=0}^{N-1} [Q(m,n)I(m+1,n) - I(m,n)Q(m+1,n)]}{\sum_{m=0}^{M-2} \sum_{n=0}^{N-1} [I(m,n)I(m+1,n) + Q(m,n)Q(m+1,n)]} \right) \right)} \quad (1)$$

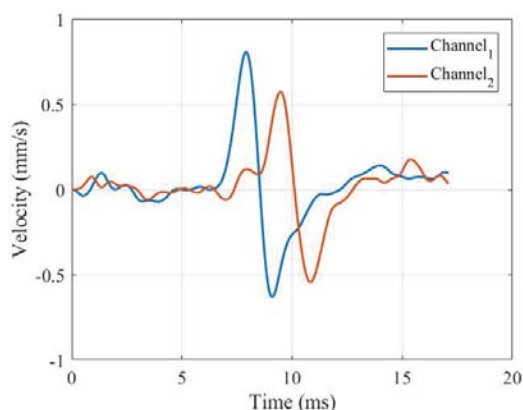


Fig. 3 Estimated tissue velocities

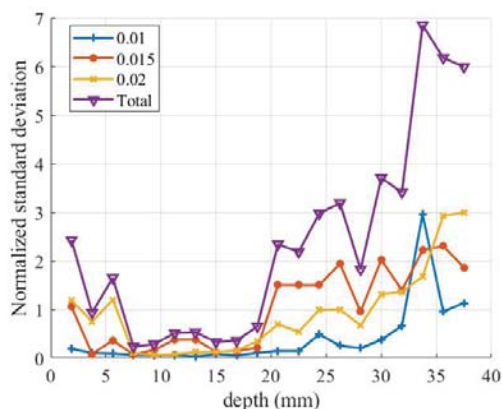


Fig. 4 Normalized standard deviation of measurement versus depth

III. RESULTS

Fig. 3 shows the transient tissue velocities corresponding to two rectangular elements, respectively. The phase delay between these two curves demonstrates the transmission of the shear waves.

As shown in Fig. 4, normalized standard deviations of measurements on three phantoms varied with the depth and their sum reach two smallest values at depths of 7.5 mm and 15 mm.

As shown in Tables I and II, values of the shear elastic modulus of three phantoms are significantly different with each other, which indicates the capability of SWE based on the three-element probe for detecting changing elasticities of soft tissues.

TABLE I
MEASURED SHEAR ELASTIC MODULUS AT THE DEPTH OF 7.5 MM

Weigh of Agar		1%	1.5%	2%
Shear elastic modulus (kPa)	Mean	8.86	23.06	36.74
	Standard deviation	0.58	1.56	3.72

TABLE II
MEASURED SHEAR ELASTIC MODULUS AT THE DEPTH OF 15 MM

Weigh of Agar		1%	1.5%	2%
Shear elastic modulus (kPa)	Mean	8.98	24.06	44.06
	Standard deviation	0.69	3.08	5.42

IV. DISCUSSIONS

To explain the phenomenon in Fig. 4 and demonstrate the effect of diffraction of ultrasound on the implementation of SWE, (3) derived from Rayleigh-Sommerfeld integral is adopted to calculate the ultrasound fields of the circular and rectangular elements

$$p(x, y, z) = jfp\mu \iint_{\Omega} \frac{1}{r} e^{-jr2\pi f/c} dx_1 dy_1 \quad (3a)$$

$$r = \sqrt{(x - x_1)^2 + (y - y_1)^2 + z^2} \quad (3b)$$

where Ω represents the area of the rectangular and circular elements, with their thickness ignored; (x, y, z) represents the location of a point at which ultrasound pressure is calculated and the origin of the coordinate is the center of each element; f is the center frequency; ρ is the density of medium; μ is the vibration velocity of particles in each element and j denotes the unit imaginary number. The variation of pressures on the axes of the two kinds of elements and the ultrasound field on the depth-lateral plane are calculated and shown in Figs. 5 and 6, respectively. It is intuitive that the pressure distribution in the ultrasound field is not uniform. The depths corresponding to two smallest values in Fig. 4 are close to the locations of two peaks between 5 mm and 15 mm in Fig. 5 respectively. Namely, the quality of the measurement is greatly affected by the diffraction of ultrasound, as a result of no beamforming processing.

The feasibility of implementing SWE by the three-element probe is verified by the experiment, which is not sufficient to evaluate the accuracy. In the future, SWE based on array probes will be used to measure the shear elastic modulus of phantoms. The ultrasound images will be generated by

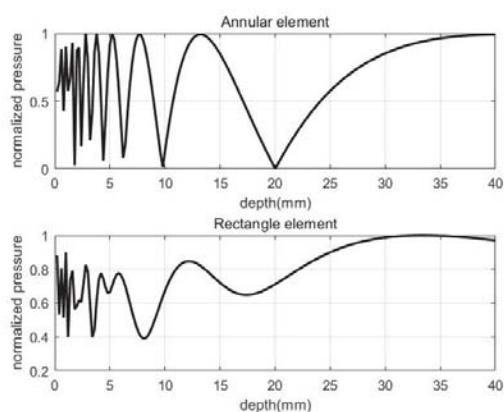


Fig. 5 Normalized pressures on the axes of the rectangular and circular elements

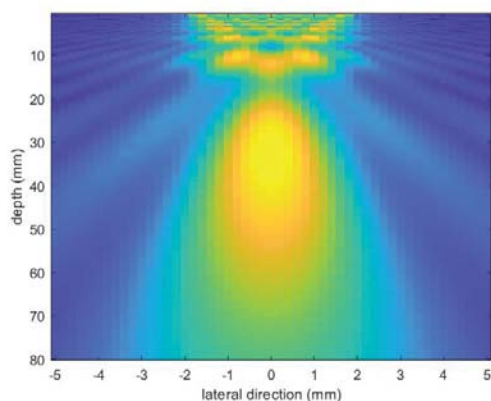


Fig. 6 Ultrasound field corresponding to the rectangular element

an array probe with and without beamforming processing respectively, to estimate errors introduced by the diffraction of ultrasound and provide a reference for designing wearable probes. The stability of generating shear waves by acoustic radiation force will be studied as well. If the variance in the generation is acceptable, there will be only one element needed for tracking and the probe can be designed with two elements, which can further improve the wearability of both the probe and equipment.

V. CONCLUSION

Morphological information detected by ultrasound can not meet the requirement of decoding human motions in some scenarios. The shear elastic modulus of skeletal muscles that was found in high correlation with human motions has the potential to cover this shortage. To realize the measurement of shear elastic modulus by wearable HMI, SWE based on the three-element probe is studied and proved to possess the ability for the measurement in this work. Future work will evaluate the accuracy of SWE based on the three-element probe and improve the design of probes.

REFERENCES

- [1] S. F. Brennan, "In vivo fascicle length measurements via b-mode ultrasound imaging with single vs dual transducer arrangements." *Journal of Biomechanics*, vol. 64, 2017.
- [2] J. Shi, "Continuous monitoring of sonomyography, electromyography and torque generated by normal upper arm muscles during isometric contraction: sonomyography assessment for arm muscles." *IEEE Transactions on Biomedical Engineering*, vol. 55, no. 3, pp. 1191–1198, 2008.
- [3] A. I. Namburete, "Computational methods for quantifying in vivo muscle fascicle curvature from ultrasound images," *Journal of Biomechanics*, vol. 44, no. 14, pp. 2538–2543, 2011.
- [4] A. I. Namburete and J. M. Wakeling, "Regional variations in fascicle curvatures within a muscle belly change during contraction." *Journal of Biomechanics*, vol. 45, no. 16, pp. 2835–2840, 2012.
- [5] J. Guo, "Dynamic monitoring of forearm muscles using one-dimensional sonomyography system," *Journal of Rehabilitation Research and Development*, 2008.
- [6] X. Yang, "Towards wearable a-mode ultrasound sensing for real-time finger motion recognition," *IEEE Transactions on Neural Systems and Rehabilitation Engineering*, vol. 26, no. 6, pp. 1199–1208, 2018.
- [7] X. Yang, J. Yan, and H. Liu, "Comparative analysis of wearable a-mode ultrasound and semg for muscle-computer interface," *IEEE Transactions on Biomedical Engineering*, pp. 1–1, 2019.
- [8] O. Maïsetti, "Characterization of passive elastic properties of the human medial gastrocnemius muscle belly using supersonic shear imaging," *Journal of Biomechanics*, vol. 45, no. 6, pp. 978–984, 2012.
- [9] K. Bouillard, "Estimation of individual muscle force using elastography," *Plos One*, vol. 6, no. 12, p. e29261, 2011.
- [10] L. Sandrin, "Shear elasticity probe for soft tissues with 1-d transient elastography," *IEEE Transactions on Ultrasonics Ferroelectrics & Frequency Control*, vol. 49, no. 4, pp. 436–446, 2002.
- [11] S. F. Eby, "Validation of shear wave elastography in skeletal muscle." *Journal of Biomechanics*, vol. 46, no. 14, pp. 2381–2387, 2013.
- [12] T. Loupas, J. T. Powers, and R. W. Gill, "An axial velocity estimator for ultrasound blood flow imaging, based on a full evaluation of the doppler equation by means of a two-dimensional autocorrelation approach," *IEEE Transactions on Ultrasonics, Ferroelectrics, and Frequency Control*, vol. 42, no. 4, pp. 672–688, 1995.
- [13] A. P. Sarvazyan, O. V. Rudenko, S. D. Swanson, J. B. Fowlkes, and S. Y. Emelianov, "Shear wave elasticity imaging: a new ultrasonic technology of medical diagnostics," *Ultrasound in Medicine & Biology*, vol. 24, no. 9, pp. 1419–1435, 1998.